Electronic Supplementary Material (ESI) for Physical Chemistry Chemical Physics.

Supporting Information:

Valence-to-Core X-Ray Emission Spectroscopy of Transition Metal Tetrahalides: Mechanisms Governing Intensity

Christina Roemelt,[a] Sergey Peredkov,[a] Frank Neese,[b] Michael Roemelt*[c] and Serena DeBeer*[a]

[a.] *Max Planck Institute for Chemical Energy Conversion, Stiftstr. 34-36, 45470 Mülheim an der Ruhr, Germany.*
[b.] *Max-Planck-Institute für Kohlenforschung, Kaiser-Wilhelm-Platz 1, 45470 Mülheim an der Ruhr, Germany.*
[c.] *Humboldt University Berlin, Brook-Taylor-Str. 2, 12489 Berlin, Germany.*

A Input files, xyz files and XES Raw Data

All input files as well as coordinate (.xyz) files, xes raw data and data needed for reproduction of figures within the manuscript can be found online: https://doi.org/10.17617/3.JECRGR

B $[MX_4]^{2-}$ Mainline Tail Fits

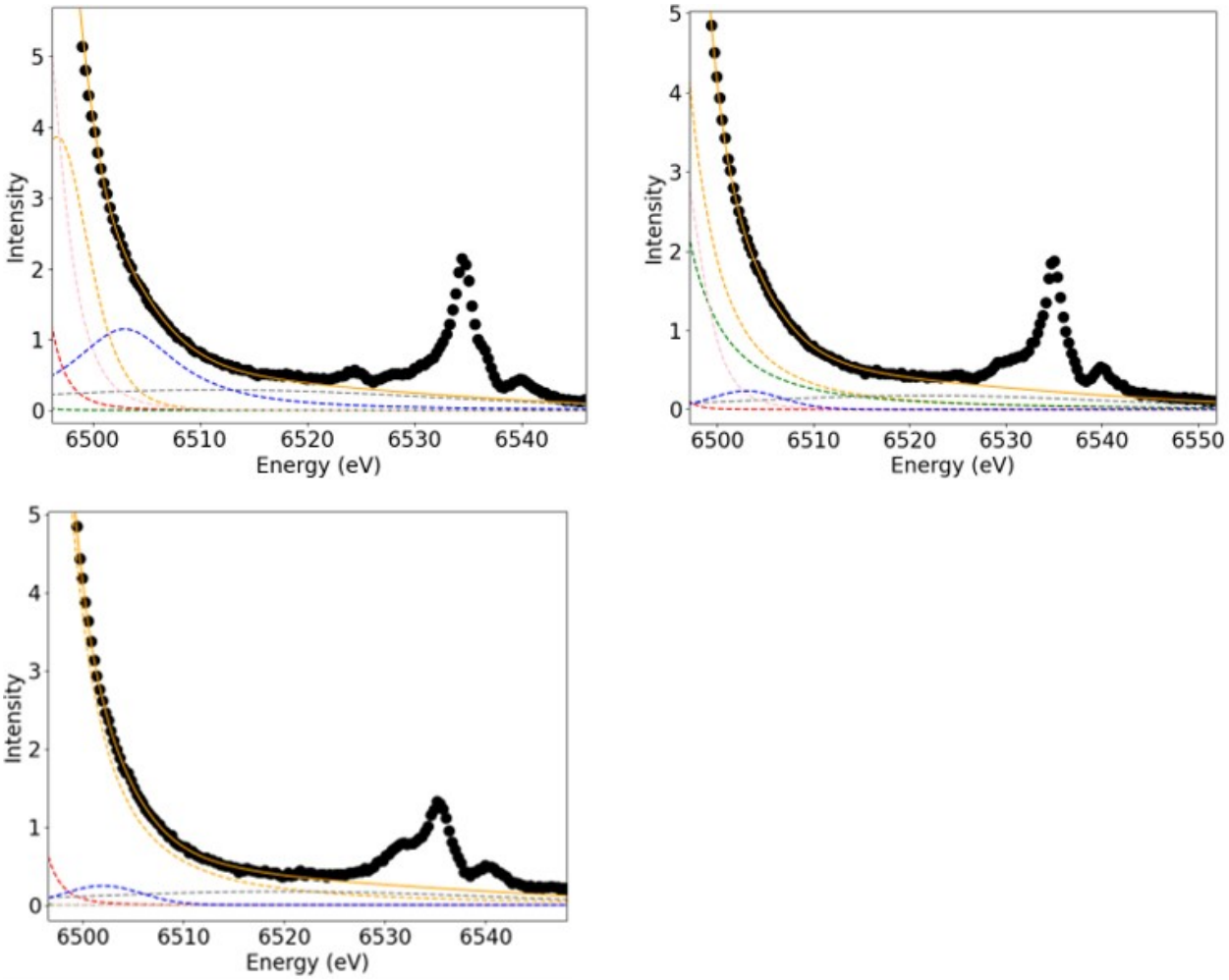

Figure S1. Mainline tail fits of the manganese halide series (top left: $[MnCl_4]^{2-}$, top right: $[MnBr_4]^{2-}$, bottom: $[MnI_4]^{2-}$). Experimental data are shown in black. The fit components are shown with colored dashed lines and the total fit is given by the solid orange line.

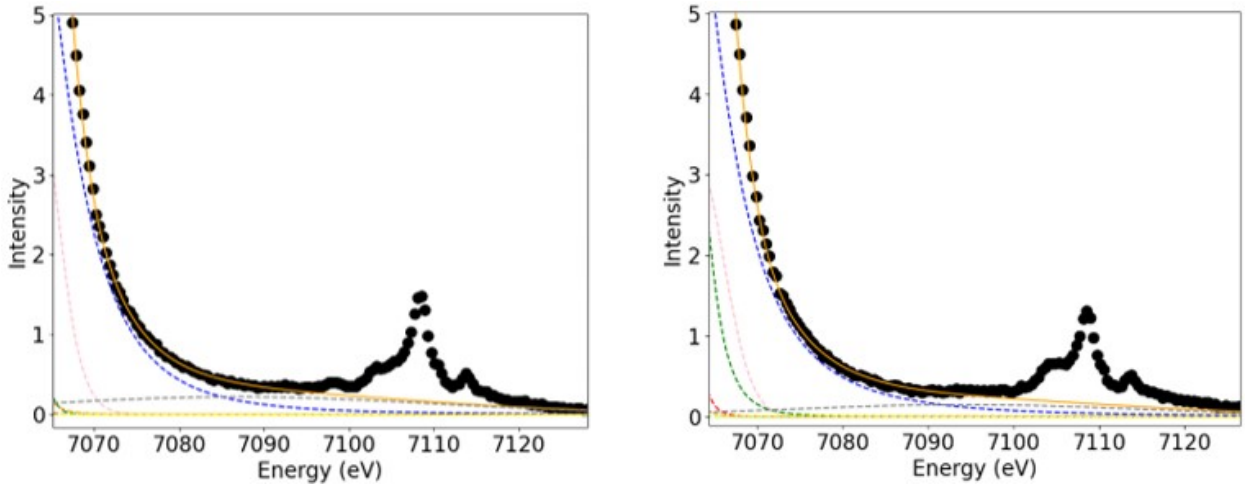

Figure S2. Mainline tail fits of the iron halide series (left: $[FeCl_4]^{2-}$, right: $[FeBr_4]^{2-}$). Experimental data are shown in black. The fit components are shown with colored dashed lines and the total fit is given by the solid orange line.

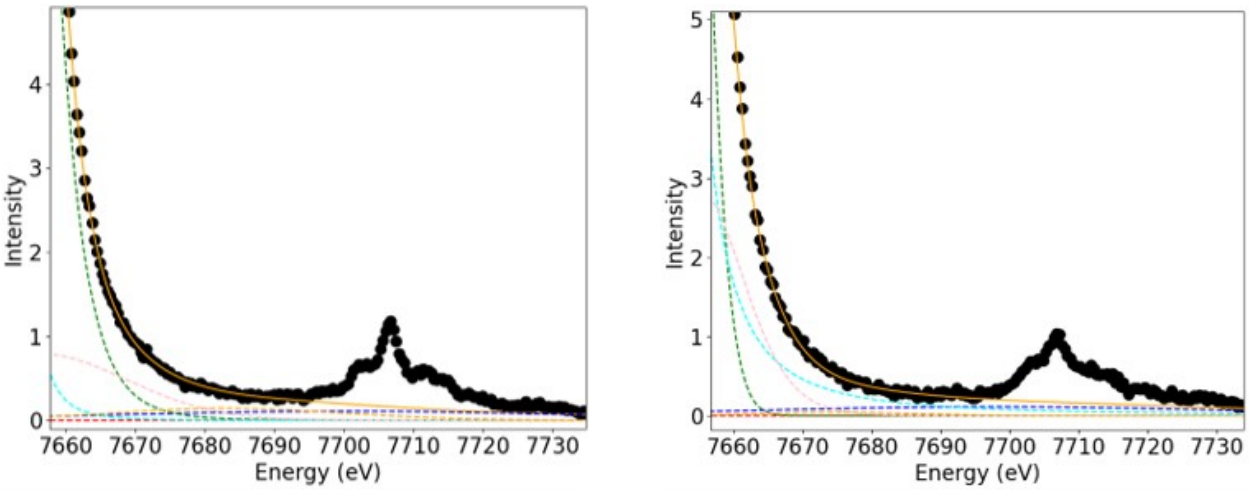

Figure S3. Mainline tail fits of the cobalt halide series (left: $[CoCl_4]^{2-}$, right: $[CoBr_4]^{2-}$). Experimental data are shown in black. The fit components are shown with colored dashed lines and the total fit is given by the solid orange line.

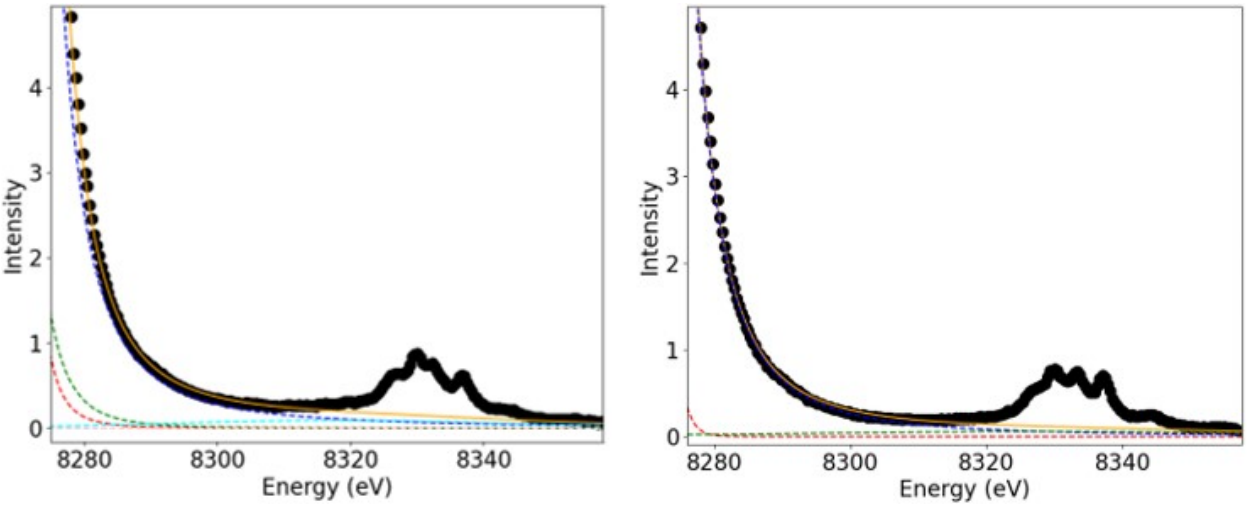

Figure S4. Mainline tail fits of the nickel halide series (left: $[NiCl_4]^{2-}$, right: $[NiBr_4]^{2-}$). Experimental data are shown in black. The fit components are shown with colored dashed lines and the total fit is given by the solid orange line.

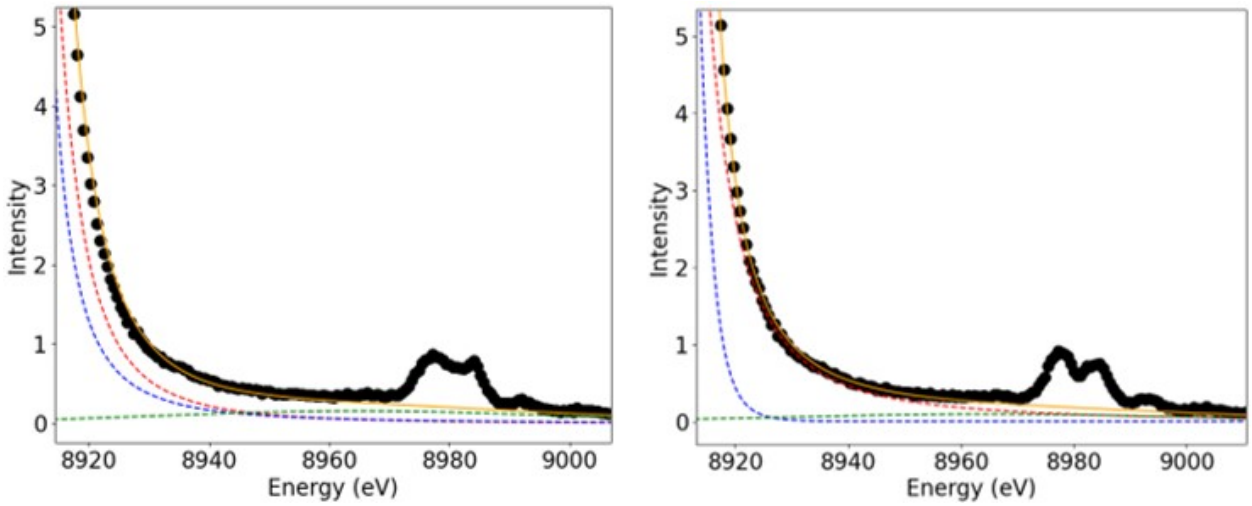

Figure S5. Mainline tail fits of the copper halide series (left: $[CuCl_4]^{2-}$, right: $[CuBr_4]^{2-}$). Experimental data are shown in black. The fit components are shown with colored dashed lines and the total fit is given by the solid orange line.

C VtC fits

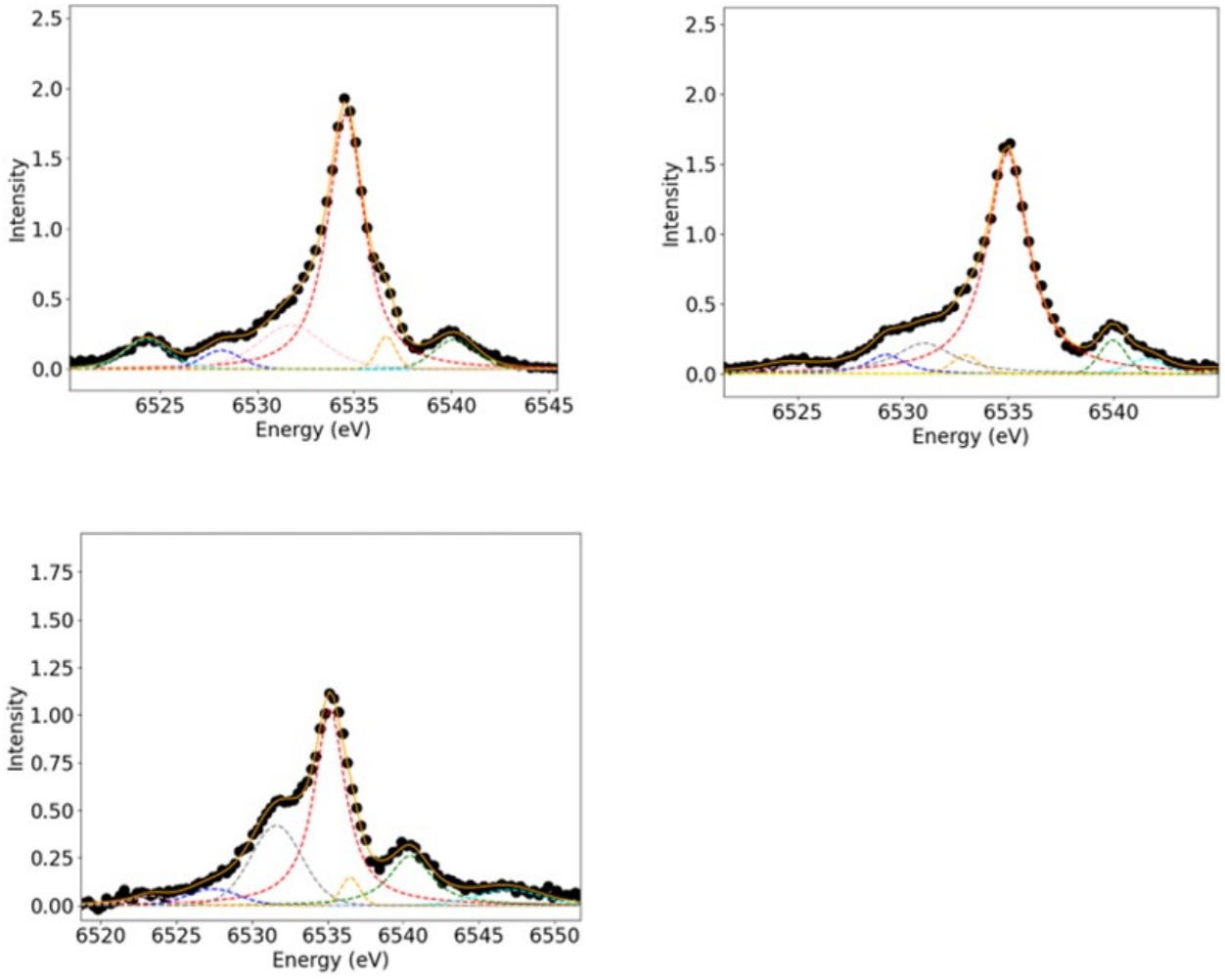

Figure S6. VtC fits of the manganese halide series (top left: $[MnCl_4]^{2-}$, top right: $[MnBr_4]^{2-}$, bottom: $[MnI_4]^{2-}$). Experimental data are shown in black. The fit components are shown with colored dashed lines and the total fit is given by the solid orange line.

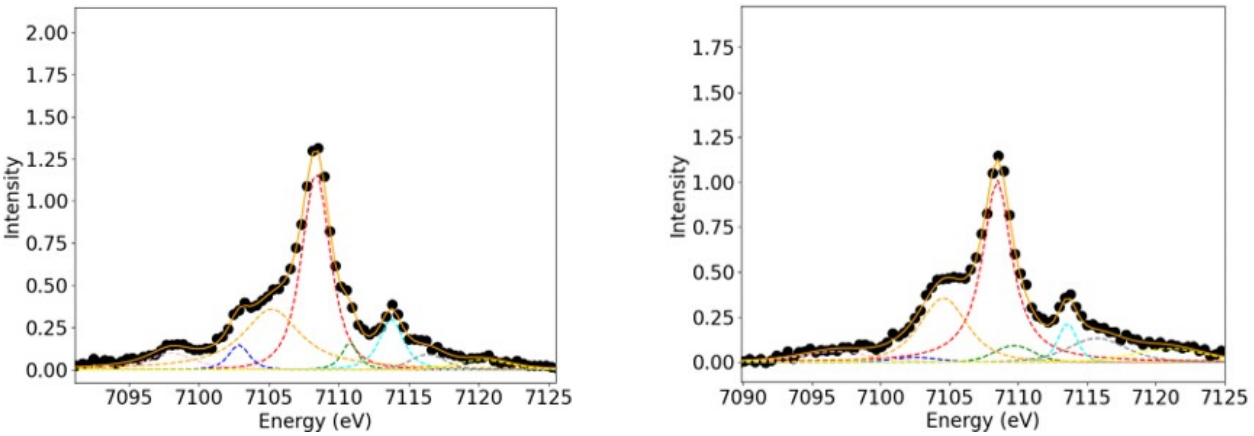

Figure S7. VtC fits of the iron halide series (left: $[FeCl_4]^{2-}$, right: $[FeBr_4]^{2-}$). Experimental data are shown in black. The fit components are shown with colored dashed lines and the total fit is given by the solid orange line.

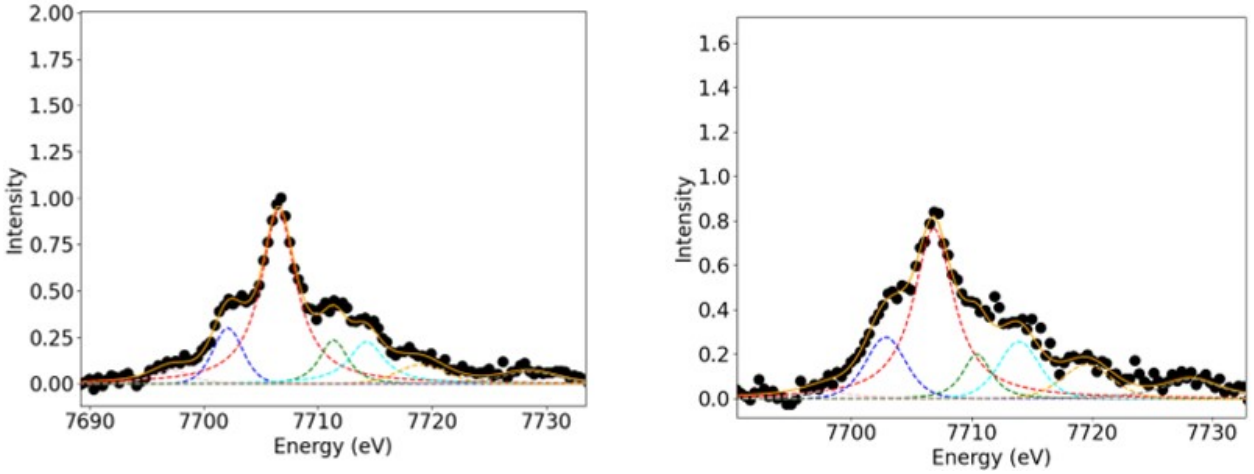

Figure S8. VtC fits of the cobalt halide series (left: $[CoCl_4]^{2-}$, right: $[CoBr_4]^{2-}$). Experimental data are shown in black. The fit components are shown with colored dashed lines and the total fit is given by the solid orange line.

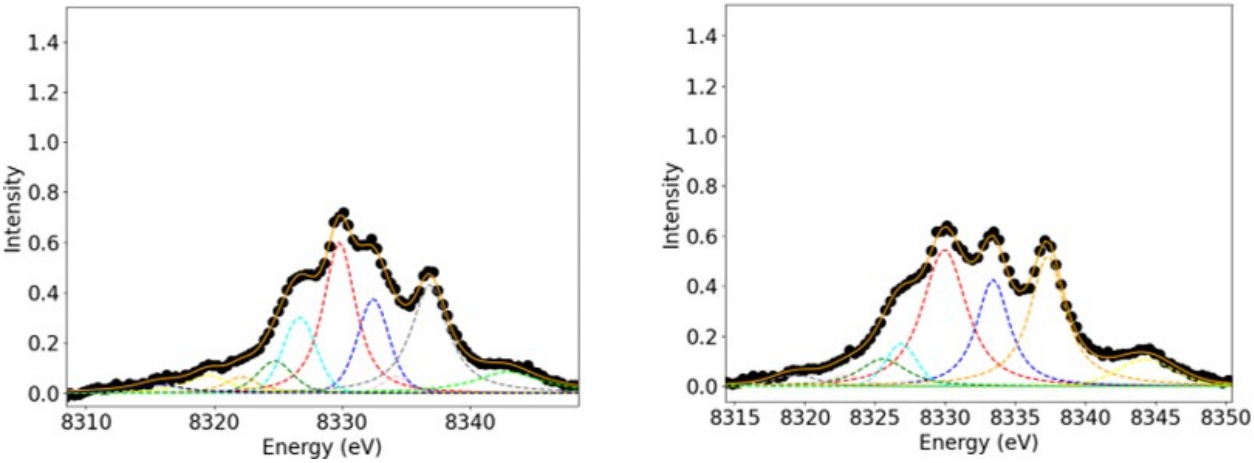

Figure S9. VtC fits of the nickel halide series (left: $[NiCl_4]^{2-}$, right: $[NiBr_4]^{2-}$). Experimental data are shown in black. The fit components are shown with colored dashed lines and the total fit is given by the solid orange line.

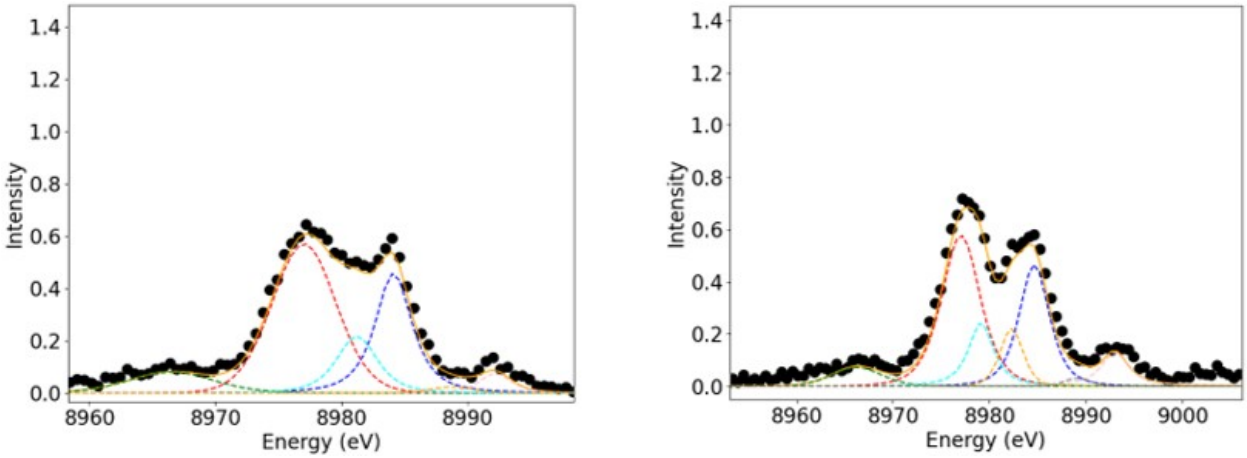

Figure S10. VtC fits of the copper halide series (left: $[CuCl_4]^{2-}$, right: $[CuBr_4]^{2-}$). Experimental data are shown in black. The fit components are shown with colored dashed lines and the total fit is given by the solid orange line.

D Correlation of p Contribution vs. Oscillator Strength For Loewdin Population Analysis (left) Compared to LCAO Analysis (right) For The Exemplary $[MnCl_4]^{2-}$ Molecule

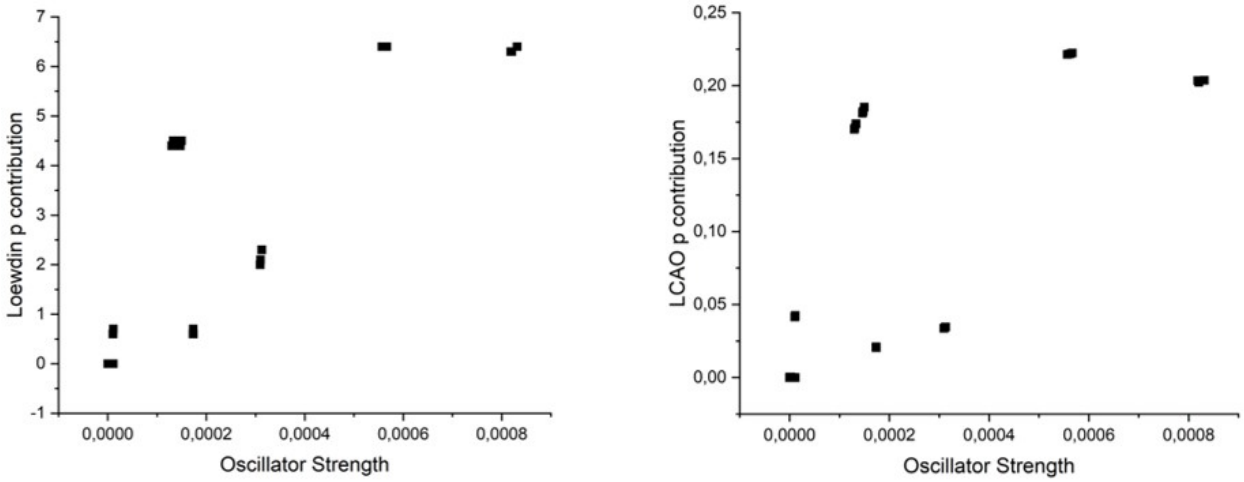

Figure S11. Loewdin p contribution (left) and LCAO p contribution (right) *vs.* oscillator strength for the exemplary $[MnCl_4]^{2-}$ molecule.

E Comparison of the LCAO 3p and 4p Contribution For The Exemplary $[MnCl_4]^{2-}$ Molecule

Peak region	MO´s contributing to VtC intensity	Mn 3p contribution to MO	Mn 4p contribution to MO
Kβ´´	30α	$1.6*10^{-5}$	0,174
	31α	$1.6*10^{-5}$	0,171
	32α	$1.6*10^{-5}$	0,17
	30β	$3.8*10^{-5}$	0,185
	31β	$3.8*10^{-5}$	0,182
	32β	$3.7*10^{-5}$	0,181
$Kβ_{2,5}$	33α	$1.1*10^{-5}$	0,02
	34α	$1.1*10^{-5}$	0,021
	35α	$1.1*10^{-5}$	0,021
	34β	$4.0*10^{-5}$	0,204
	35β	$3.9*10^{-5}$	0,202
	36β	$3.9*10^{-5}$	0,203
	39α	$9.8*10^{-6}$	0,222
	40α	$9.7*10^{-6}$	0,222
	41α	$9.6*10^{-6}$	0,221
	39β	$1.2*10^{-8}$	0,041
	40β	$1.5*10^{-8}$	0,042
	41β	$1.7*10^{-8}$	0,042
	47α	$3.4*10^{-6}$	0,034
	48α	$3.4*10^{-6}$	0,034
	49α	$3.4*10^{-6}$	0,035

F Definition of the Transition Dipole Moment And Relation to Oscillator Strength

According to Fermi's golden rule, the intensity of an electronic transition from initial state $|\psi_I\rangle$ to final state $|\psi_F\rangle$ is proportional to the square of corresponding transition dipole moment, i.e.

$$I_{IF} \propto \left|\langle\psi_I\left|\vec{\hat{\mu}}\right|\psi_F\rangle\right|^2 \qquad (1)$$

The dipole operator has incorporated positions and charges from all nuclei and electrons:

$$\vec{\hat{\mu}} = \sum_A Q_A \vec{R}_A - \sum_i \vec{r}_i \qquad (2)$$

As all positions $\vec{R}_A$ and $\vec{r}_i$ are vectors in position space with 3 components each, $\vec{\hat{\mu}}$ is a vectorial quantity, too. The three components

$$T_{IF}^x = \langle\langle\psi_I\left|\hat{\mu}_x\right\rangle\left|\psi_F\right\rangle \qquad (3)$$

$$T_{IF}^y = \langle\langle\psi_I\left|\hat{\mu}_y\right\rangle\left|\psi_F\right\rangle \qquad (4)$$

$$T_{IF}^z = \langle\langle\psi_I\left|\hat{\mu}_z\right\rangle\left|\psi_F\right\rangle \qquad (5)$$

are the transition dipole moments along the *x*, *y* and *z* axes, respectively. However, the right hand side of equation (1) incorporates the square of $\vec{\hat{\mu}}$ which is the sum of the square of all three vector components, i.e.

$$I_{IF} \propto \left|T_{IF}^{x}\right|^2 + \left|T_{IF}^{y}\right|^2 + \left|T_{IF}^{z}\right|^2 \tag{6}$$

In case of transition metal K-edge VtC spectroscopy, the initial state corresponds to a core excited ionized state with a hole in the 1s shell of the transition metal while in the final state said core hole is filled by a valence electron. When two-electron processes and correlation effects that would lead to the involvement of higher excited configurations are neglected, ψ_F and ψ_I consist of a single electronic configuration. In that case, the transition dipole moment between the two states reduces to a transition dipole moment between the two orbitals involved in aforementioned electronic transition:

$$\left|\langle\psi_I\left|\vec{\hat{\mu}}\right|\psi_F\rangle\right| \approx \left|\langle\Phi_p\left|\vec{\hat{\mu}}\right|1s\rangle\right| \tag{7}$$

Here $|\Phi_p\rangle$ denotes the valence orbital involved in the VtC transition and $|1s\rangle$ is the transition metal 1s orbital.

The transition dipole moment μ_i of a transition is related to the oscillator strength *f* of the transition via

$$f = \frac{2m_e\Delta E}{3\hbar^2 e^2}|\mu_i|^2 \tag{8}$$

where m_e is the mass of the electron, ΔE is the energy of the transition, $\hbar$ is the reduced Planck constant and *e* is the charge of the electron.